Theor. Comput. Fluid Dyn. (2023) 37:627–637
https://doi.org/10.1007/s00162-023-00662-1

ORIGINAL ARTICLE

Youngjin Hwang · Sangkwon Kim · Chaeyoung Lee · Soobin Kwak · Gyeonggyu Lee · Junseok Kim

Monte Carlo simulation of the coffee-ring effect on porous papers

Received: 30 August 2022 / Accepted: 2 June 2023 / Published online: 15 June 2023

Abstract In this article, we present a mathematical model and numerical simulation of the coffee-ring effect on porous papers. The numerical method is based on Monte Carlo simulation. The proposed model is simple but can capture the main mechanism of coffee stain formation on porous papers. Several numerical experiments are presented to demonstrate the performance of the proposed algorithm. We can obtain the coffee-ring effect on porous papers as the computer simulation results.

Keywords Coffee-ring effect · Monte Carlo simulation · Computer simulation · Numerical algorithm

1 Introduction

When a droplet containing solutes evaporates on a solid substrate, the solutes deposit onto the substrate in a coffee-ring pattern. Experimental results by Pham and Kumar have shown that substrate permeability can inhibit coffee-ring patterns and lead to more uniform solute deposition [1]. Recently, various studies on models and theories for the uniform deposition of nanoparticles have been conducted. Theoretical and numerical simulations of the scaling laws of two Newtonian droplets coalescence were performed [2]. Katiyar and Singh [3] studied molecular dynamics to understand the self-assembly of nanoparticles upon the evaporation of nanofluid droplets on their surface. The self-assembled structure of nanoparticles is affected by several factors, such as the size and shape of the nanoparticles, the solvent-surface, and the nanoparticle–surface interaction strengths. Zhang et al. [4] investigated two factors, nanoparticle–liquid interaction strength and evaporation rate, on the formation and structure of nanoparticle deposits produced after drying nanoscale droplets on a solid surface. The model developed in [5] has demonstrated that it is possible to simulate the formation of streaks on the surface of the interior of a container by the coffee-ring effect with the evaporation rate. Wang and Nestler [6] proposed the numerical discretization of Cahn's wetting transition model to study the wetting transition and phase separation on flat substrates and porous structures. The absorption of liquids through porous media is highly important in many scientific processes and industrial applications such as printing, textiles, agriculture, and blood diagnostic apparatus [7]. The coffee-ring effect caused by the non-uniform particle distribution of porous paper creates various problems in scientific processes, industrial applications, and nanotechnology fields. Therefore, Yu et al. [8] and Oh et al. [9] presented a method for suppressing the coffee-ring effect by uniformly distributing particles on porous paper in inkjet printing technology. Controlled reduction of the coffee-ring effect significantly improves the profile of inkjet-printed Ag electrodes. Printing conditions, such as drop spacing, the printing layer, and substrate temperature, can control the coffee-ring

Communicated by Stefania Cherubini.

Y. Hwang · S. Kim and C. Lee · S. Kwak · G. Lee · J. Kim (✉)
Department of Mathematics, Korea University, Seoul 02841, Republic of Korea
E-mail: cfdkim@korea.ac.kr

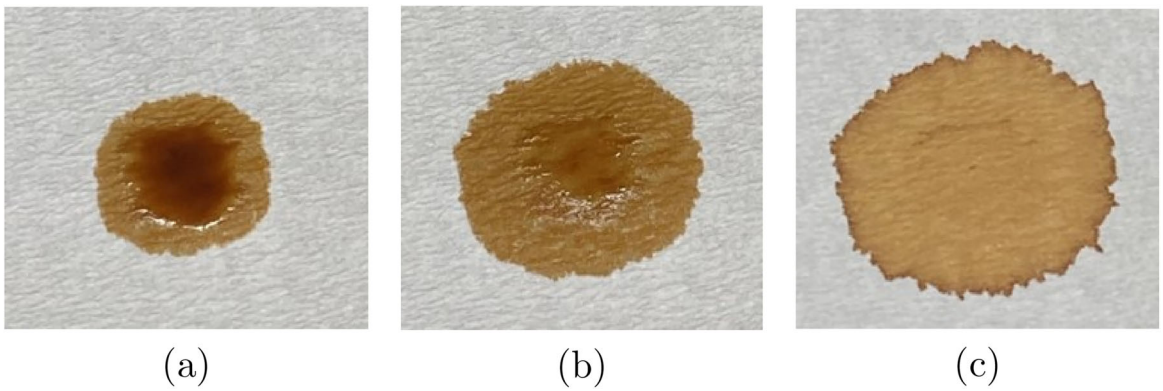

Fig. 1 Temporal evolution of coffee stain on a porous paper

effect, and by finding the optimal printing conditions, the coffee-ring effect is greatly reduced, improving the profiles of inkjet-printed electrodes [10]. Park et al. [11] proposed a stable and easy simulation that modifies various parameters to reduce the coffee-ring effect.

If coffee is spilled on porous paper, a coffee-ring may be left behind at the boundary of the spill. Understanding this phenomenon is useful for controlling material transport in porous papers [12]. In general, although the coffee-ring effect on the stain formation at the edge of the droplet by droplet wicking is relatively well known, the phenomenon of staining at the center of the droplet by the Marangoni flow is sometimes observed [13]. In addition, whilst the drying of a sessile drop through evaporation can result in the development of Marangoni flows that may counteract the radial flow associated with coffee staining, the process of drying through capillary drainage does not have the ability to generate such flows [14]. Therefore, in this paper, we generally ignore the Marangoni flow and consider only droplet wicking.

The coffee solution spilt on the paper can be seen in Fig. 1a. Figure 1b shows the process of diffusion of dropped coffee solution on the paper. The coffee stain that became deposit state after the diffusion phenomenon stopped can be found in Fig. 1c. Nilghaz et al. [12] investigated the pattern of coffee stains on porous paper and the underlying mechanism of stain formation. Stain formation on the paper can be utilized to quantify the kinetics of antibody-red blood cell (RBC) stain formation for blood typing diagnostics [15]. The coffee-ring effect on the distribution and transport of red blood cells in the porous cellulose fiber network has been studied and known [16]. This investigation provides a fundamental technique for governing RBCs on porous paper materials and designing of paper-based clinical diagnostics. In general, the structure of paper is porous, therefore, the liquid falling on the paper spreads by droplet wicking by capillary action [15,16].

The main objective of this paper is to propose a mathematical model based on Monte Carlo simulation (MCS) for the coffee-ring effect on porous papers and to demonstrate its performance through computational simulations. Thus far, experimental studies have been conducted on various solid substrate conditions to investigate methods for suppressing the coffee-ring effect. Zhang et al. [17] experimentally investigated the evaporation and patterns of colloidal droplets on glass slide substrates with different roughness and found that roughness affects the evaporation of droplets. He and Derby [18] considered the coffee-ring effect on Si/SiO_2 substrates by inkjet printing. Cho et al. [19] demonstrated the influence of porous alumina nanostructures. Previously, a model to comprehend the inter-particulate activities of the coffee-ring effect was lacking. A discrete element model (particle system) was developed to investigate the coffee-ring effect, and it was found that the internal Marangoni flow was not required for suppression of the coffee-ring effect [20]. The Brownian motion, which represents the random motion of particles, has been used to represent the motion of particles in particle transport devices [21] and is also used in models to investigate the onset of double-diffusion convection in a layer of magnetic nanofluid [22]. In this paper, we use Monte Carlo simulations and Brownian motion to represent the motion of coffee particles. Amraui et al. demonstrated that the antiperovskite $ZnFe_3N$ presents metallic behavior according to the electronic density of state and band structure shape using ab-initio calculation and Monte Carlo simulation in [23]. Shin et al. [24] presented a method for estimating the electron energy spectra based on the singular value decomposition of the detector response function, and demonstrated the method of calculating instrument response function with MCS under the penetration of charged particles. Moha et al. simulated electron trajectories to determine the optimum combination of quantum well structure and a node voltage using MCS in [25].

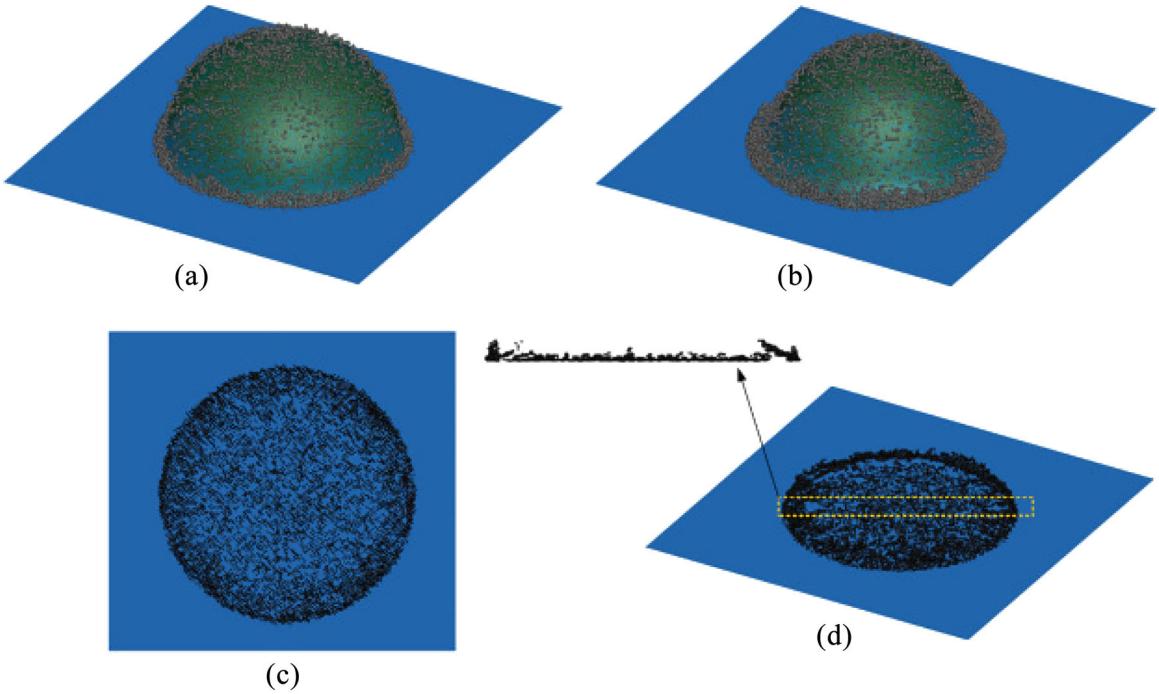

Fig. 2 Droplet evaporation on a solid substrate with particles. Reprinted from [26] with permission from Elsevier Publishing

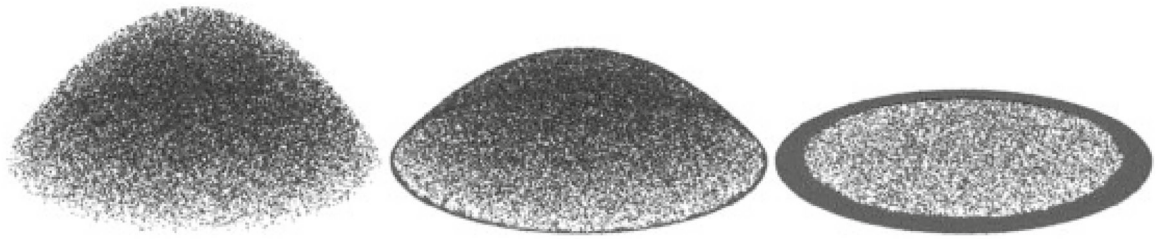

Fig. 3 Droplet evaporation on a solid substrate with particles Reprinted from [28] with permission from Elsevier Publishing

In this study, we present a mathematical model and perform a Monte Carlo simulation of the coffee-ring effect on porous papers. In many studies on nanoparticles, a system of phase-field equations and Langevin equations or a system of equations of fluid dynamics and Langevin equations are constructed to solve the problem of the dynamics of particles in droplets on a solid substrate in three-dimensional space [26–29]. See Figs. 2 and 3 for the computational results using numerical methods [26,28].

The coffee ring effect due to droplet evaporation on a substrate causes a coffee stain inside the initial droplet due to the pinning boundary condition of the droplet. That is, the coffee particles inside the droplet do not migrate outside the area of the pinned droplet. Unlike droplets on substrates, droplets on porous paper can be absorbed into the paper, and there is no pinning boundary and particles can escape the initial droplet region [12,16,30]. Fu et al. [30] used the volume of the fluid model to accurately track droplet deformation and presented a pressure implicit split operator algorithm to compute the coupling of droplet pressure and velocity. Ezzatneshan and Goharimehr [31] proposed an algorithm to predict multiphase flow properties and interfacial dynamics influenced by the interaction between a droplet and a multi-phase substrate based on the multiphase lattice Boltzmann method. Numerical methods for sessile droplet spreading and penetration on porous substrates are important for investigating the physical mechanism of the spreading and imbibition of a droplet into fibrous porous membranes. The developed numerical methods for droplets on porous substrates focused on the interaction between droplets and porous media, therefore, they cannot observe the movement of particles inside the droplets, or they have limitations in not being able to simulate multiple droplets because of axisymmetry. Consequently, it was difficult to observe the coffee ring effect on a porous substrate through numerical experiments. The coffee ring model presented in this paper can simulate the important characteristics

of porous paper simply and efficiently for single and multiple droplets, enabling a more intuitive understanding of the interparticle activity.

The contents of this paper are as follows. In Sect. 2, we describe the governing equation and numerical solution algorithm. The computational experiments are given in Sect. 3. Finally, conclusions are presented in Sect. 4.

2 Governing equation and numerical solution algorithm

The coffee particles move according to a random walk with a truncated standard normal distribution under gravitational force [29]. The governing equation can be derived from the Langevin equation on the two-dimensional domain $\Omega = (L_x, R_x) \times (L_y, R_y)$:

$$\frac{\mathrm{d}\mathbf{X}}{\mathrm{d}t} = \frac{\alpha}{\sqrt{\mathrm{d}t}}\psi(\mathbf{X}) \text{ on } \Omega, \tag{1}$$

where $\mathbf{X}$ is Lagrangian variable for a particle, t is time, and α is diffusion coefficient. Here, $\psi(\mathbf{X}) = (\beta_1\rho\cos(\theta), \beta_2\rho\sin(\theta))$ represents random force of the Brownian particle, where ρ and θ are the random variables. The random variable ρ has a mean of 0 and a variance of 1 in the closed interval $[a, b]$ and θ has a value between 0 and 2π. The weights β_1 and β_2 for the x-axis and y-axis are based on a biased random walk to consider the structure of the porous paper [32]. $\sqrt{\mathrm{d}t}$ is constructed by variance in a Wiener process for time t. Please refer to the reference for more details [33]. The truncated normal distribution with the probability density function f [34]:

$$f(\rho) = \frac{\phi(\rho)}{\Phi(b) - \Phi(a)}, \text{ for } a \le \rho \le b; \quad f = 0 \text{ otherwise.} \tag{2}$$

where $a = -2.576, b = 2.576$. a and b represent 99.7% confidence value. The parameters ϕ and Φ are the standard normal distribution and the cumulative distribution function, respectively. Using the explicit Euler's method, we discretize Eq. (1) as

$$\frac{\mathbf{X}_{k,d}^{n+1} - \mathbf{X}_{k,d}^{n}}{\Delta t} = \frac{\alpha}{\sqrt{\Delta t}}\psi(\mathbf{X}_{k,d}^{n}), \quad k = 1, 2, \ldots, N_p, \tag{3}$$

where $\mathbf{X}_{k,d}^{n}$ is the k-th particle position at time $t = n\Delta t$. Here, Δt is the time step and N_p is the number of particles. The total number of particles N_p for the same area physically means the droplet density, and time step Δt can be used in proportion to N_p. The subscript d represents the particle status, i.e., $d = 0$ is dried and $d = 1$ is wetted. Equation (3) can be rewritten as

$$\mathbf{X}_{k,d}^{n+1} = \mathbf{X}_{k,d}^{n} + \alpha\sqrt{\Delta t}\psi(\mathbf{X}_{k,d}^{n}), \quad k = 1, 2, \ldots, N_p. \tag{4}$$

Let us define a discrete wetted particle R-neighborhood of $\mathbf{X}_{k,d}^{n}$ as

$$\mathcal{N}_R(\mathbf{X}_{k,d}^{n}) = \left\{ \mathbf{X}_{p,1}^{n} \mid \quad \mid \mathbf{X}_{k,d}^{n} - \mathbf{X}_{p,1}^{n} \mid < R, \quad 1 \le p \le N_p \right\}.$$

In addition, $\#\left(\mathcal{N}_R(\mathbf{X}_{k,d}^{n})\right)$ denotes the cardinality of the set $\mathcal{N}_R(\mathbf{X}_{k,d}^{n})$.

The movement of nanoparticles depends on the interaction strength, the closest distance of approach, and the distance between two particles [3]. In addition, depending on the pore size of the porous paper, the interaction strength of capillary action will change, which can increase or decrease coffee stains [14]. Therefore, the proposed algorithm repeats the below two steps until all particles become a dry state.

- State update: If there are not enough wetted particles in the R_1-neighborhood of $\mathbf{X}_{k,1}^{n}$, i.e., $\#\left(\mathcal{N}_{R_1}(\mathbf{X}_{k,1}^{n})\right) \le M_1$, then $\mathbf{X}_{k,1}^{n}$ becomes a dried particle $\mathbf{X}_{k,0}^{*}$; otherwise it remains as a wetted particle, $\mathbf{X}_{k,1}^{*} = \mathbf{X}_{k,1}^{n}$.
  Here, M_1 and R_1 are status parameters representing the degree of drying of water droplets by evaporation and the degree of absorption by capillarity of porous paper, respectively. If the value of M_1 is large, the particle evaporates and dries quickly. If the value of R_1 is small, the capillary action strength, which represents the interaction with the paper, is strong, resulting in fast permeation

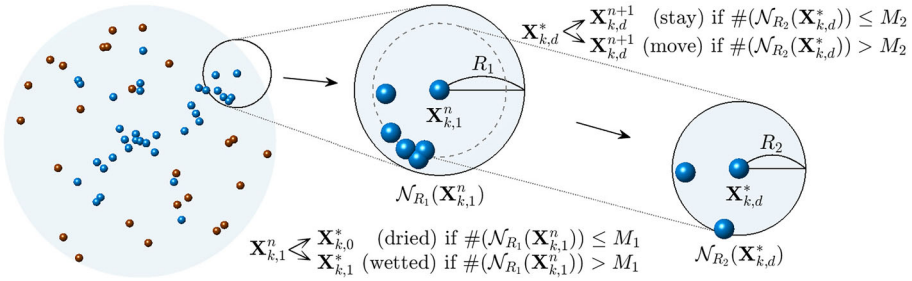

Fig. 4 Schematic illustration of the proposed algorithm

- Move or stay: If there are enough wetted particles in the R_2-neighborhood of $\mathbf{X}^*_{k,d}$, i.e., $\#\left(\mathcal{N}_{R_2}(\mathbf{X}^*_{k,d})\right) \ge M_2$, then $\mathbf{X}^*_{k,d}$ moves next time according to Eq. (4), $\mathbf{X}^{n+1}_{k,d} = \mathbf{X}^*_{k,d} + \alpha\sqrt{\Delta t}\psi(\mathbf{X}^*_{k,d})$; otherwise it stays, $\mathbf{X}^{n+1}_{k,d} = \mathbf{X}^*_{k,d}$.

Here, M_2 and R_2 are the movement parameters for interaction strength and closest distance of approach that will cause the wet particle to move, respectively. The smaller the value of M_2, the fewer wet particles are required for the movement interaction, and the higher the value of R_1, the wider the closest distance of approach that can interact with the particle, allowing more particles to move (Fig. 4).

3 Computational experiments

In this section, we perform several numerical simulations using the proposed algorithm with different parameter values to observe the coffee-ring effect on porous papers.

3.1 Convergence test

To observe the effect of time step, temporal evolution is observed for each time step $\Delta t = 0.8, 0.4, 0.2$ and 0.1. Figure 5 shows the computational results with different time step size at $t = 256$. The parameters are used as following: $R_1 = 0.3$, $R_2 = 0.06$, $\Delta t = 0.1$, $\alpha = 0.2$, $\beta_1 = 1$, $\beta_2 = 1$, $N_p = 5000$, $M_1 = 5$ and $M_2 = 1$. The initial position of $\mathbf{X}^0_{k,1}$ for $k = 1, \ldots, N_p$ are randomly distributed in a circle centered at $(0, 0)$ and $r = 0.5$. The computational result converges as we refine the time step. Thus, we use the time step Δt as 0.1.

3.2 Effect of the state criteria M_1

We perform numerical experiments to observe the effect of the coffee-ring on the state criterion value M_1, which is required to update the state of the particle. The parameters for the numerical simulation are: $R_1 = 0.3$, $R_2 = 0.06$, $\Delta t = 0.1$, $\alpha = 0.2$, $\beta_1 = 1$, $\beta_2 = 1$, $N_p = 5000$, and $M_2 = 1$. The initial position of the particle $\mathbf{X}^0_{k,1}$ for $k = 1, \ldots, N_p$ are randomly distributed in a circle with a center of $(0, 0)$ and a radius of 0.5. We use a fixed movement criterion value $M_2 = 1$, such that all wetted particles are always moving. The numerical experiments are performed until the particles are in equilibrium when $M_1 = 5$.

Figure 6a, b shows the temporal evolution of the coffee-ring effect for different $M_1 = 2$ and 5, respectively. From left to right, times are at $t = 0,\ 250\Delta t,\ 500\Delta t$, and $1863\Delta t$. Here, the last time $1863\Delta t$ is the time at which all particles are dry and in equilibrium when $M_1 = 5$. In the case of $M_1 = 5$, if the number of wetted particles in the R_1-neighborhood of wetted particle $\mathbf{X}^*_{k,1}$ for $k = 1, \ldots, N_p$ is 5 or less, it is changed to dried particle $\mathbf{X}^*_{k,0}$. Therefore, it is difficult to maintain the state of the wetted particles. Because the number of wetted particles in R_1-neighborhood which require the state of the wetted particles is relatively larger than that in the case of $M_1 = 2$. Comparing the effect of the state criterion value M_1 at $t = 250\Delta t$, we observed that wet particles changed to dried particles relatively quickly when $M_1 = 5$ compared to when $M_1 = 2$. In the case of $M_1 = 2$ at time $t = 1863$, contrary to the equilibrium state observed when $M_1 = 5$, wet particles still existed and the particles were diffusing.

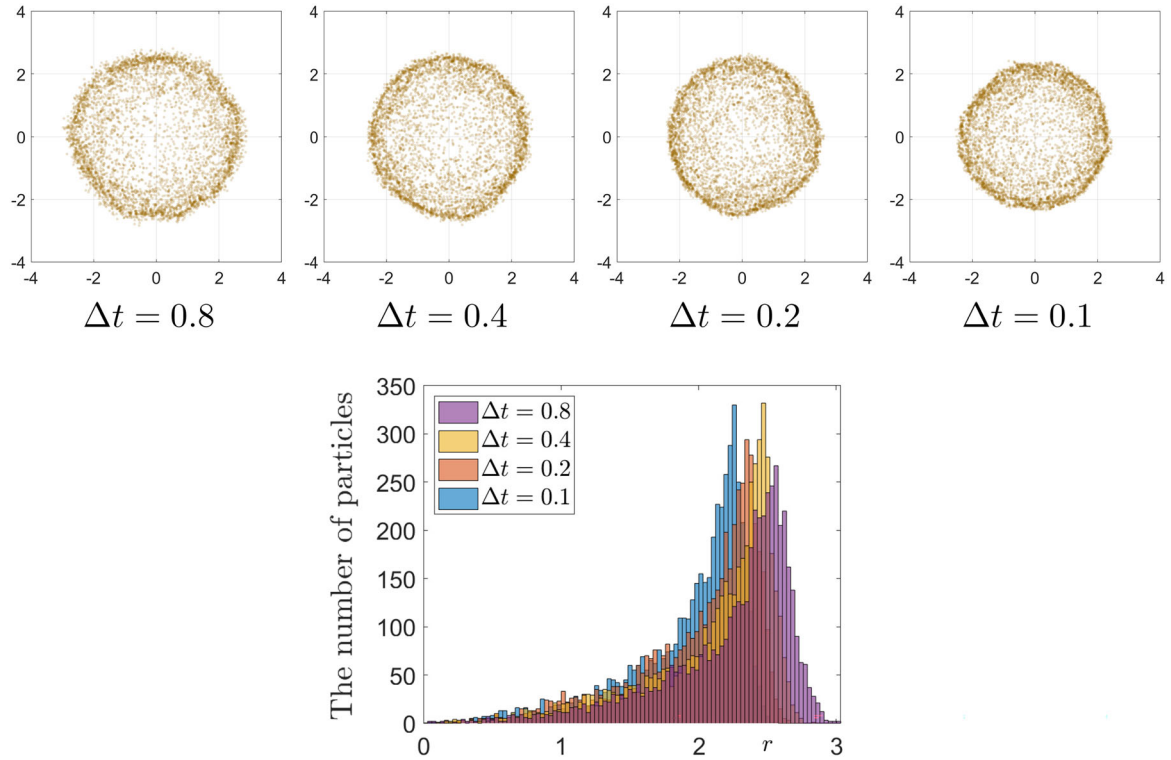

Fig. 5 The first row is the computational results with different time step size Δt at $t = 256$. The second row is histogram of the number of particles at $t = 256$

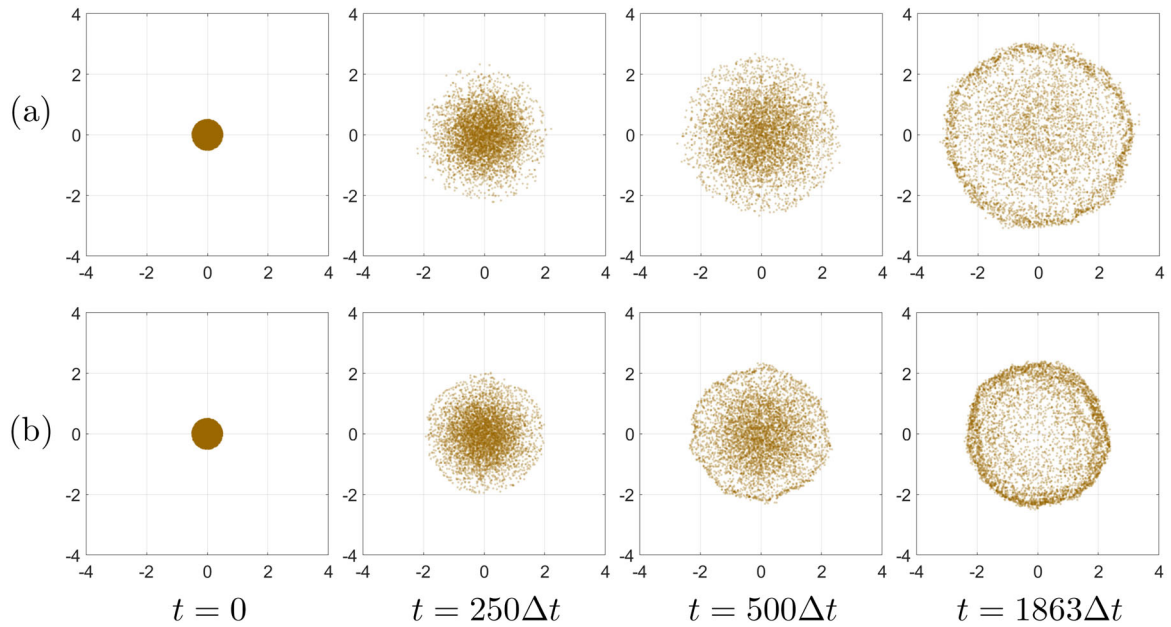

Fig. 6 Temporal evolution of coffee-ring pattern formation with different M_1 values: **a** $M_1 = 2$, **b** $M_1 = 5$. Here, $M_2 = 1$ is used

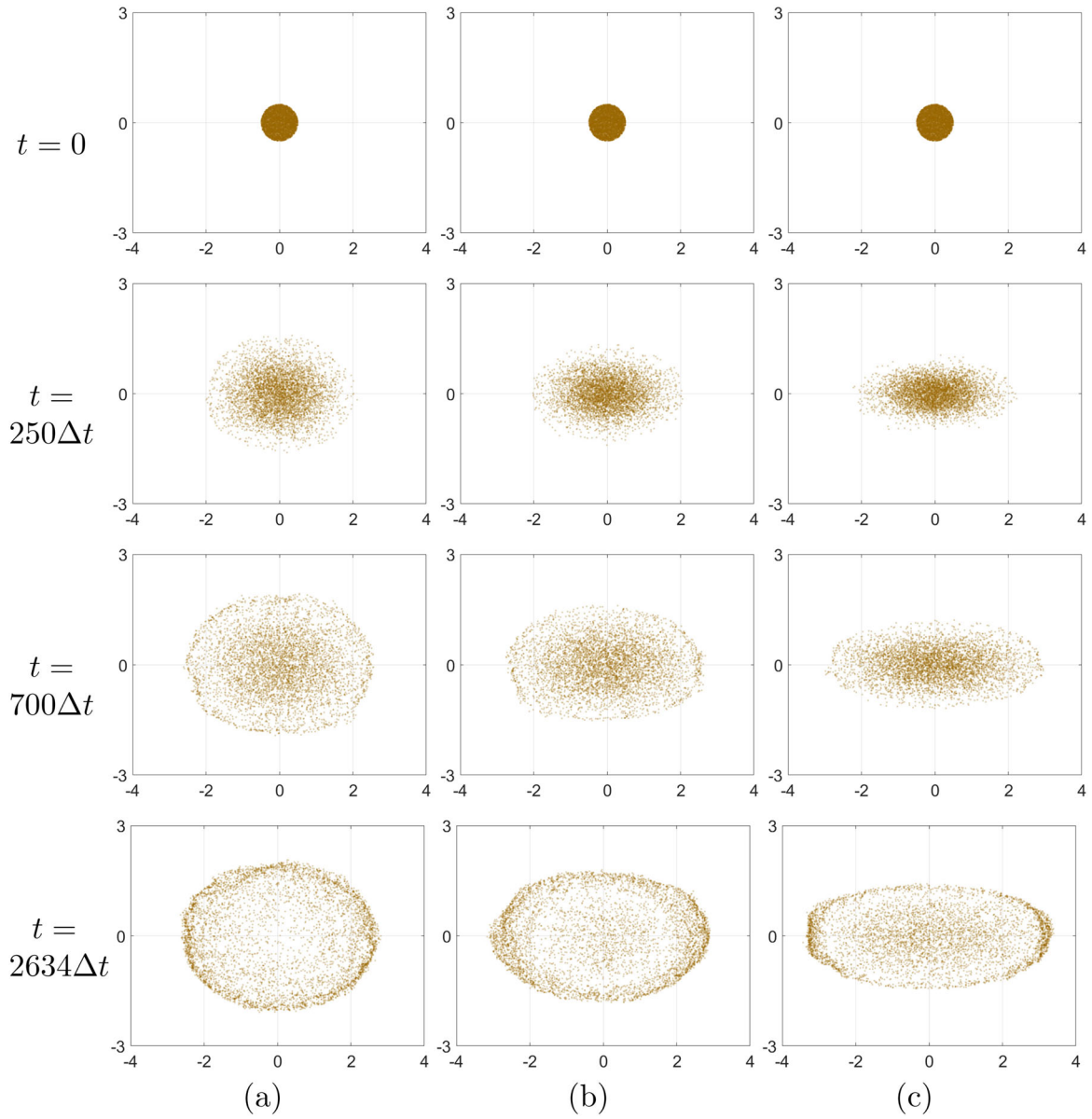

Fig. 7 Temporal evolution of coffee-ring pattern formation with different $\psi(\mathbf{X})$ values: **a** $\psi(\mathbf{X}) = (\rho\cos(\theta), 0.7\rho\sin(\theta))$, **b** $\psi(\mathbf{X}) = (\rho\cos(\theta), 0.5\rho\sin(\theta))$, and **c** $\psi(\mathbf{X}) = (\rho\cos(\theta), 0.3\rho\sin(\theta))$

3.3 Effect of the paper structure

We perform numerical simulations to observe the effect of paper structure on the coffee-ring effect. The proposed algorithm presents the coffee-ring effect by droplet wicking on porous paper. The coffee droplet is absorbed along the direction of the fiber of the porous paper and the coffee-ring effect appears. Therefore, the coffee-ring effect may appear in different shapes depending on the characteristics of the fibers of the porous paper that meet the droplets. The initial position of the particles $\mathbf{X}_{k,1}^0$ for $k = 1, \ldots, N_p$ are randomly distributed in a circle with a center of $(0, 0)$ and a radius of 0.5. The initial parameters are $R_1 = 0.3$, $R_2 = 0.06$, $\Delta t = 0.1$, $\alpha = 0.2$, $\beta_1 = 1$, $N_p = 5000$, $M_1 = 5$, $M_2 = 1$, and different parameters $\beta_2 = 0.7, 0.5, 0.3$.

Figure 7a–c illustrates the numerical simulation results by varying $\psi(\mathbf{X}) = (\rho\cos(\theta), \beta_2\rho\sin(\theta))$ of the algorithm to observe the coffee-ring effect by droplet wicking on porous paper, where β_2 is proportional to the vertical capillary action of the porous paper. Here, the last time $2634\Delta t$ is the time at which all particles are dry and in equilibrium when $\beta_2 = 0.7$. We can observe that the coffee-ring effect is formed in a horizontally

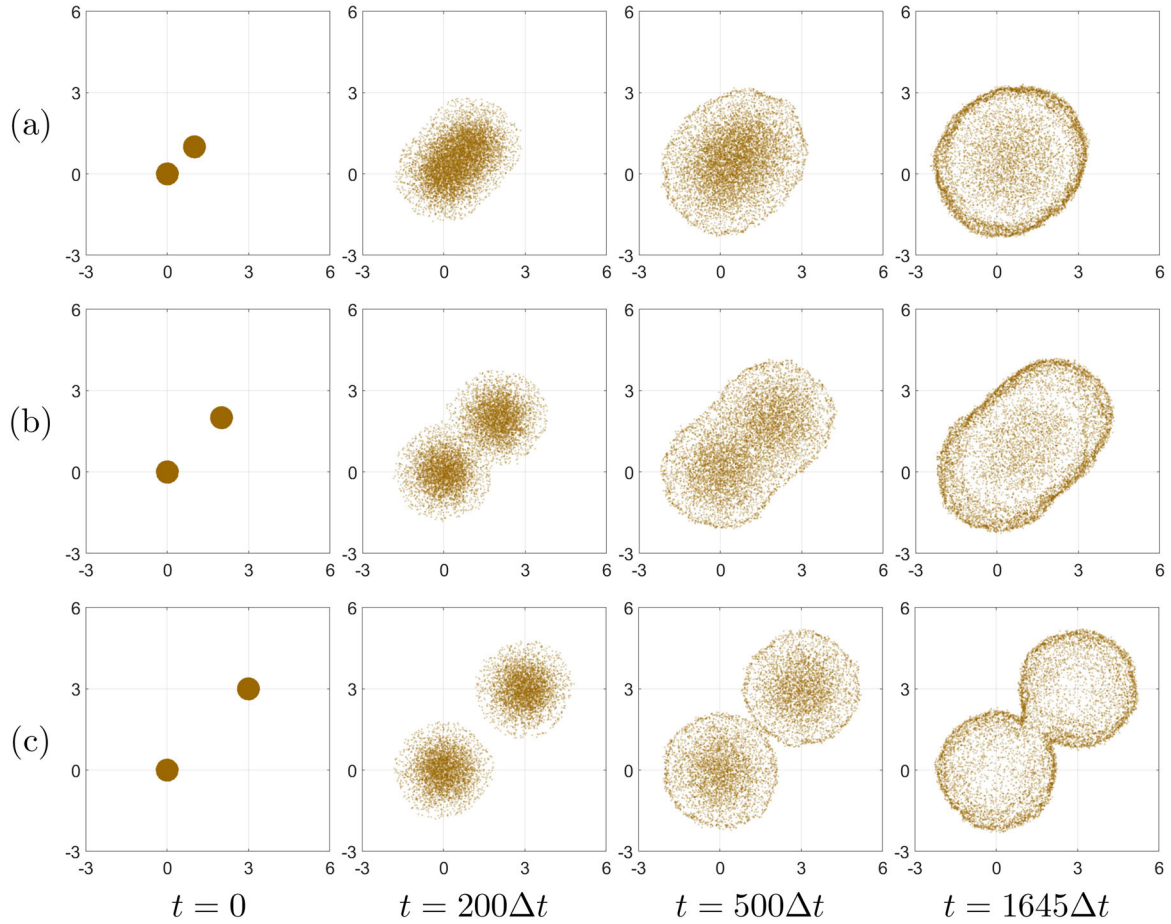

Fig. 8 The temporal evolution of coffee-ring pattern formation when the first droplet and second droplet with different center points (c_1, c_2) fall at the same time. **a** $c_1 = 1, c_2 = 1$, **b** $c_1 = 2, c_2 = 2$, and **c** $c_1 = 3, c_2 = 3$

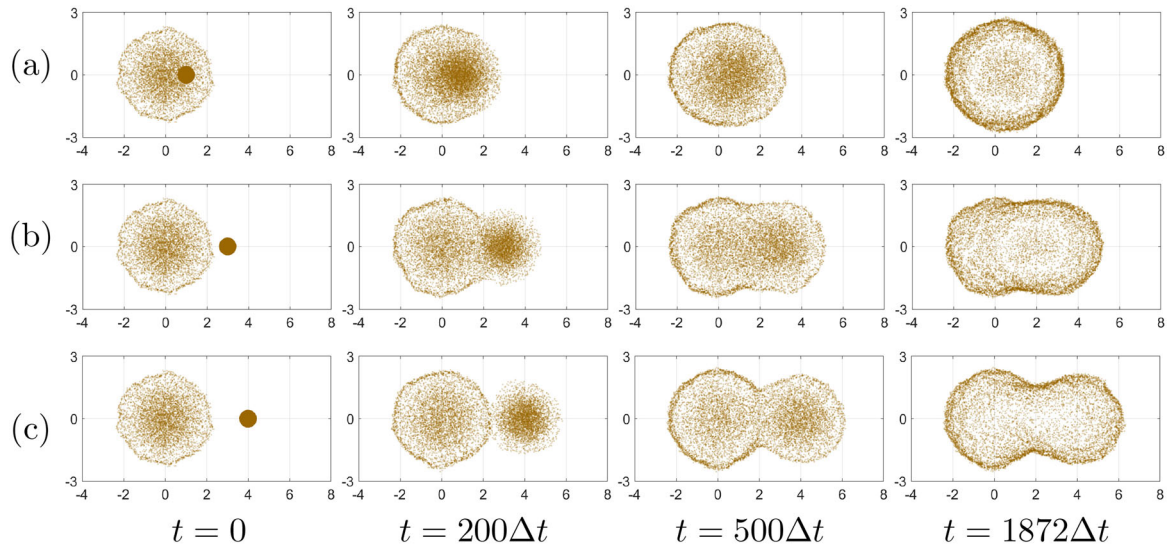

Fig. 9 Temporal evolution of coffee-ring pattern formation for when new droplet with different center points (c_1, c_2) is dropped before all particles of the first droplet are dried. **a** $c_1 = 1, c_2 = 0$, **b** $c_1 = 3, c_2 = 0$, and **c** $c_1 = 4, c_2 = 0$

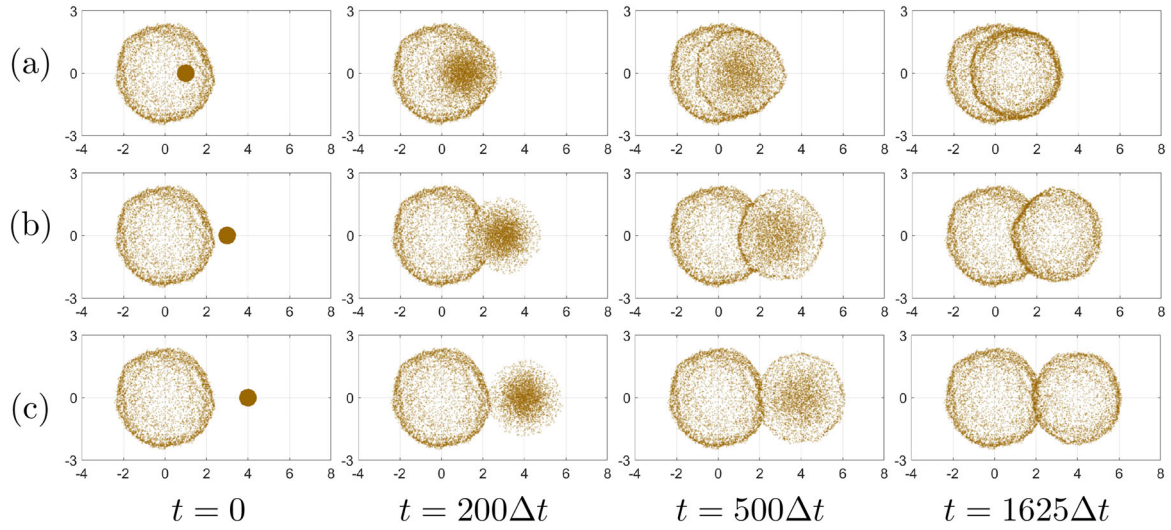

Fig. 10 Temporal evolution of coffee-ring pattern formation for when new droplet with different center points (c_1, c_2) is dropped after all particles of the first droplet are dried. **a** $c_1 = 1, c_2 = 0$, **b** $c_1 = 3, c_2 = 0$, and **c** $c_1 = 4, c_2 = 0$

long elliptical pattern. When β_2 is less than 1, the horizontal droplet wicking in the porous paper was greater than the vertical droplet wicking.

3.4 Multi-droplets

The coffee-ring effect in the porous paper is that even if all the particles of one droplet are dried and are in equilibrium, when a new droplet is dropped on it, the dried particles can be moved by the wet particles. Therefore, we perform the coffee-ring effect for multi-droplets. For numerical simulation, the initial position of particles $\mathbf{X}_{k,1}^0, k = 1, \ldots, N_p$ for the first droplet are randomly distributed in a circle with a center of $(0, 0)$ and a radius of r, and initial position of particles $\hat{\mathbf{X}}_{\hat{k},1}^0, \hat{k} = 1, \ldots, \hat{N}_p$ for second droplet are randomly distributed in a circle with a center of (c_1, c_2) and a radius of $\hat{r}$. Unless otherwise, we use the parameters $R_1 = 0.3$, $R_2 = 0.06$, $\Delta t = 0.1$, $\alpha = 0.2$, $\beta_1 = 1$, $\beta_2 = 1$, $M_1 = 5$, $M_2 = 1$.

First, we perform a computational simulation to observe the coffee-ring effect when two drops fall at the same time. The considered parameters are $N_p = 4000$, $\hat{N}_p = 4000$, different center points $(c_1, c_2) = (1, 1), (2, 2), (3, 3)$ of second droplet, $r = 0.4$ and $\hat{r} = 0.4$. Here, the last time $1645\Delta t$ is the time at which all particles are dried and in equilibrium state when $c_1 = 3, c_2 = 3$. Figure 8a–c shows the particle diffusion of two droplets over the time for different center points $(1, 1), (2, 2), (3, 3)$ of the second droplet, respectively.

Second, we perform the computational experiments to observe the coffee-ring effect caused by dropping the new droplet before all particles of the first droplet are dried. We use the case of $M_1 = 5$ at $t = 500\Delta t$, which is one of the numerical experimental results at Sec. 3.2, as the initial condition of the first droplet. This is the result in Fig. 6b when $t = 500\Delta t$. The used parameters are: $N_p = 5000$, $\hat{N}_p = 4000$, different center points $(c_1, c_2) = (1, 0), (3, 0), (4, 0)$ of second droplet, $r = 0.5$, and $\hat{r} = 0.4$. Here, the last time $1872\Delta t$ is the time at which all particles are dried and in equilibrium state when $c_1 = 4, c_2 = 0$. Figure 9 shows the coffee-ring pattern formation for when new droplet with different center points (c_1, c_2) is dropped before all particles of the first droplet are dried. We observed that the wetted particles of the first droplet interacted with the wetted particles of the second droplet to diffuse and there was no boundary between the different droplets.

Third, numerical simulation is performed to observe the coffee-ring effect when a new droplet falls after all particles of the first droplet are dried. We use the case of $M_1 = 5$ at $t = 1863\Delta t$, which is one of the numerical experimental results at Sec. 3.2, as the initial condition of the first droplet. This is the numerical result in Fig. 6b when $t = 1863\Delta t$. Thus, all particles of the first droplet are dried. However, even if all of the particles are dried, they can move if new droplets fall and wetted particles are formed. For numerical simulation, we used parameters that are $N_p = 5000$, $\hat{N}_p = 4000$, different center points $(c_1, c_2) = (1, 0), (3, 0), (4, 0)$ of second droplet, $r = 0.5$, and $\hat{r} = 0.4$. Here, the last time $1625\Delta t$ is the time at which all particles are dried

and in equilibrium state when $c_1 = 4$, $c_2 = 0$. In Fig. 10, we can observe the movement of dried particles by the wetted particles of new droplets after all particles of the first droplet are dried, and the coffee-ring pattern formation accordingly. In the coffee-ring pattern formed, the boundary between the first droplet and the second droplet is clearly observed, unlike the results of the second simulation shown in Fig. 9. In addition, comparing the last time t of the second and third simulations, the drying time of all particles was faster when the second droplet fell after all the particles of the first droplet were dried.

4 Conclusions

In this study, we presented a mathematical model and numerical simulation of the coffee-ring effect on porous papers using Monte Carlo simulation. The proposed model is very simple but can capture the main mechanism for coffee stain formation by droplet wicking on a porous paper. In the numerical experiments, we can confirmed the performance of the proposed algorithm for coffee-ring formation by droplet wicking on a porous paper. In addition, we presented the multi-droplet effect by various numerical experiments. Here, we consider the difference in time and distance for each droplet. In future research work, we plan to further investigate the effect of the anisotropic fiber network of porous papers. Furthermore, it is difficult to fit the physical parameters in numerical simulation without a real experiment. Therefore, we consider checking physical parameters and fitting for numerical simulation with a real experiment as future work.

Acknowledgements The corresponding author (J.S. Kim) was supported by Korea University Grant. The authors would like to thank the reviewers for their valuable suggestions and comments to improve this manuscript.

Declarations

Author contributions Hwnag wrote the main manuscript text and all the authors reviewed and discussed the manuscript.

Conflict of interest The authors declare that they have no conflicts of interest.

Data availability The data used to support the findings of this study are included in the article.

References

1. Pham, T., Satish, K.: Imbibition and evaporation of droplets of colloidal suspensions on permeable substrates. Phys. Rev. Fluids **4**(3), 034004 (2019)
2. Khodabocus, M.I., Sellier, M., Nock, V.: Scaling laws of droplet coalescence: theory and numerical simulation. Adv. Math. Phys. **2018**, 4906016 (2018)
3. Katiyar, P., Singh, J.K.: Evaporation induced self-assembly of different shapes and sizes of nanoparticles: a molecular dynamics study. J. Chem. Phys. **150**(4), 044708 (2019)
4. Zhang, J., Milzetti, J., Leroy, F., Müller-Plathe, F.: Formation of coffee-stain patterns at the nanoscale: the role of nanoparticle solubility and solvent evaporation rate. J. Chem. Phys. **146**(11), 114503 (2017)
5. Kim, H., Yang, J., Kim, S., Lee, C., Yoon, S., Kwak, S., Kim, J.: Numerical simulation of the coffee-ring effect inside containers with time-dependent evaporation rate. Theor. Comput. Fluid Dyn. **66**, 1–11 (2022)
6. Wang, F., Nestler, B.: Wetting transition and phase separation on flat substrates and in porous structures. J. Chem. Phys. **154**(9), 094704 (2021)
7. Hertaeg, M.J., Tabor, R.F., Garnier, G.: Effect of protein adsorption on the radial wicking of blood droplets in paper. J. Colloid Interface Sci. **528**, 116–123 (2018)
8. Yu, X., Xing, R., Peng, Z., Lin, Y., Du, Z., Ding, J., Wang, L., Han, Y.: To inhibit coffee ring effect in inkjet printing of light-emitting polymer films by decreasing capillary force. Chin. Chem. Lett. **30**(1), 135–138 (2019)
9. Oh, Y., Kim, J., Yoon, Y.J., Kim, H., Yoon, H.G., Lee, S.N., Kim, J.: Inkjet printing of Al2O3 dots, lines, and films: from uniform dots to uniform films. Curr. Appl. Phys. **11**(3), S359–S363 (2011)
10. Liu, C.F., Lin, Y., Lai, W.Y., Huang, W.: Improved performance of inkjet-printed Ag source/drain electrodes for organic thin-film transistors by overcoming the coffee ring effects. AIP Adv. **7**(11), 115008 (2017)
11. Park, Y., Park, Y., Lee, J., Lee, C.: Simulation for forming uniform inkjet-printed quantum dot layer. J. Appl. Phys. **125**(6), 065304 (2019)
12. Nilghaz, A., Zhang, L., Shen, W.: Coffee stains on paper. Chem. Eng. Sci. **129**, 34–41 (2015)
13. Baek, J.M., Yi, C., Rhee, J.Y.: Central spot formed in dried coffee-water-mixture droplets: inverse coffee-ring effect. Curr. Appl. Phys. **18**(4), 477–483 (2018)
14. Dou, R., Derby, B.: Formation of coffee stains on porous surfaces. Langmuir **28**(12), 5331–5338 (2012)
15. Hertaeg, M.J., Tabor, R.F., McLiesh, H., Garnier, G.: A rapid paper-based blood typing method from droplet wicking. Analyst **146**(3), 1048–1056 (2021)

16. Cao, R., Pan, Z., Tang, H., Wu, J., Tian, J., Nilghaz, A., Li, M.: Understanding the coffee-ring effect of red blood cells for engineering paper-based blood analysis devices. Chem. Eng. J. **391**, 123522 (2020)
17. Zhang, Y., Chen, X., Liu, F., Li, L., Dai, J., Liu, T.: Enhanced coffee-ring effect via substrate roughness in evaporation of colloidal droplets. Adv. Condens. Matter Phys. **2018**, 9795654 (2018)
18. He, P., Derby, B.: Controlling coffee ring formation during drying of inkjet printed 2D inks. Adv. Mater. Interfaces **4**(22), 1700944 (2017)
19. Cho, H., Kim, S.M., Liang, H., Kim, S.: Electric-potential-induced uniformity in graphene oxide deposition on porous alumina substrates. Ceram. Int. **46**(10), 14828–14839 (2020)
20. Xu, T., Lam, M.L., Chen, T.H.: Discrete element model for suppression of coffee-ring effect. Sci. Rep. **7**(1), 42817 (2017)
21. Bradshaw-Hajek, B.H., Islam, N., Miklavcic, S.J., White, L.R.: Convective and diffusive particle transport in channels of periodic cross-section: comparison with experiment. J. Eng. Math. **111**(1), 1–13 (2018)
22. Mahajan, A., Sharma, M.K.: Double-diffusive convection in a magnetic nanofluid layer with cross diffusion effects. J. Eng. Math. **115**(1), 67–87 (2019)
23. Amraoui, S., Feraoun, A., Kerouad, M.: Theoretical study of the magnetic and magnetocaloric properties of the $ZnFe_3N$ antiperovskite. Curr. Appl. Phys. **31**, 68–73 (2021)
24. Shin, Y., Na, G.W., Seon, J.: Estimation of electron fluxes in the Earth's geostationary orbit with Tikhonov regularization during a magnetically quiet period. Curr. Appl. Phys. **31**, 246–253 (2021)
25. Mohan, M., Shim, S., Cho, M., Kim, T., Kwak, J., Park, J., Jang, N., Ryu, S., Lee, N., Lee, J.: Ultraviolet–cathodoluminescent 330 nm light source from a 2-inch wide CNT electron-beam emission under DC electric field. Curr. Appl. Phys. **28**, 72–77 (2021)
26. Zhang, L., Wang, X.: Numerical coffee-ring patterns with new interfacial schemes in 3D hybrid LB–LE model. Powder Technol. **392**, 130–140 (2021)
27. Crivoi, A., Duan, F.: Three-dimensional Monte Carlo model of the coffee-ring effect in evaporating colloidal droplets. Sci. Rep. **4**(1), 1–6 (2014)
28. Breinlinger, T., Kraft, T.: A simple method for simulating the coffee stain effect. Powder Technol. **256**, 279–284 (2014)
29. Yang, J., Kim, H., Lee, C., Kim, S., Wang, J., Yoon, S., Kim, J.: Phase-field modeling and computer simulation of the coffee-ring effect. Theor. Comput. Fluid Dyn. **34**(5), 679–692 (2020)
30. Fu, F., Li, P., Wang, K., Wu, R.: Numerical simulation of sessile droplet spreading and penetration on porous substrates. Langmuir **35**(8), 2917–2924 (2019)
31. Ezzatneshan, E., Goharimehr, R.: Study of spontaneous mobility and imbibition of a liquid droplet in contact with fibrous porous media considering wettability effects. Phys. Fluids **32**(11), 113303 (2020)
32. Codling, E.A., Bearon, R.N., Thorn, G.J.: Diffusion about the mean drift location in a biased random walk. Ecology **91**(10), 3106–3113 (2010)
33. Schulten, K., Kosztinm, I.: Lectures in Theoretical Biophysics, p. 117. University of Illinois (2000)
34. Botev, Z.: The normal law under linear restrictions: simulation and estimation via minimax tilting. J. R. Stat. Soc. Ser. B Stat. Methodol. **79**(1), 125–148 (2017)